Contents available at: Sri Lanka Journals Online

Tropical Agricultural Research

Journal Home Page: https://tar.sljol.info

RESEARCH

Investigation of Accuracy for Rice Crop Parameters Predicted Using UAV Multispectral Imagery

P.P. Dharmaratne[1]*, A.S.A. Salgadoe[1], W.M.U.K. Rathnayake[2] and A.D.A.J.K. Weerasinghe[3]

[1]*Department of Horticulture and Landscape Gardening, Faculty of Agriculture and Plantation Management, Wayamba University of Sri Lanka, Makandura, Gonawila, 60170, Sri Lanka*
[2]*Rice Research and Development Institute, Bathalagoda, Ebbagamuwa, 60500, Sri Lanka*
[3]*Retail Information Technologies Pvt Ltd, Bambalapitiya, Sri Lanka*

ARTICLE INFO

Article history:
Received: 22 March 2024
Revised version received: 20 December 2024
Accepted: 24 December 2024
Available online: 01 January 2025

Keywords:
Farmer field
Multispectral
Pix4D mapper
UAV
Vegetation Indices

Citation:
Dharmaratne, P.P., Salgadoe, A.S.A., Rathnayake, W.M.U.K. and Weerasinghe, A.D.A.J.K. (2024). Investigation of Accuracy for Rice Crop Parameters Predicted Using UAV Multispectral Imagery. Tropical Agricultural Research, 36(1): 82-98.

DOI:
https://doi.org/10.4038/tar.v36i1.8885

Dharmaratne, P.P.
https://orcid.org/0009-0002-2739-6917

ABSTRACT

Remote measurement of rice crop parameters; Leaf-Chlorophyll, Above-ground biomass, Plant Height, Leaf Moisture and Rice Yield of rice plants before the actual harvest are vital for the early management of rice crops. This study was conducted in controlled rice fields and extended to farmer rice fields in the *Maha* season in Sri Lanka. The multispectral aerial images of the field were acquired by an Unmanned Ariel Vehicle (UAV) and processed. Vegetation indices (VIs) were then derived and selected the best combination of VIs explaining the respective ground-measured parameters. The combination of selected VIs showed significant association (R^2=0.84, RMSE=0.28; R^2=0.81, RMSE=0.06 kg/m^2; R^2=0.63, RMSE=0.11 cm; R^2=0.57, RMSE= 0.16% and R^2=0.98, RMSE=128.5 kg/ha, Leaf-Chlorophyll, Above-ground biomass, Plant height, Leaf moisture, and Rice yield respectively) with the ground data in the controlled rice field experiment conducted at the Rice Research and Development Institute (RRDI), Bathalagoda, Sri Lanka. When these selected vegetation indices were transferred to a farmer rice field they showed a relationship as R^2=0.57, RMSE=1.35; R^2=0.60, RMSE=1.23 kg/m^2; R^2=0.41, RMSE= 9.95 cm; R^2=0.36, RMSE= 34.4% and R^2=0.53, RMSE=563.04 kg/ha respectively., The vegetation indices derived from UAV-multispectral images were able to associate and estimate the rice crop parameters like Leaf-Chlorophyll, Above-ground biomass and Rice Yield at booting stage and 25 m flying height. Therefore, VIs developed using UAV multispectral imagery to measure Leaf-Chl, AGB, PHt, LM and RY behave differently across rice fields in different soils, rice varieties, weedy conditions and agronomic practices.

*Corresponding author- dharmaratnep@gmail.com

INTRODUCTION

Rice is generally grown in two cropping seasons, the *Yala* and the *Maha* which are related to the dry and wet seasons of Sri Lanka. Agro-climatically, the year is divided into two seasons coinciding with the monsoons as *Maha* and *Yala* and rice lands are cultivated in these distinct two seasons (Gitelson and Merzlyak, 1996). The major cultivation season *Maha*, which is from late September to February is fed with inter-monsoon rain and with the North-east monsoon, which is well distributed all over the island (Agudo *et al.*, 2018; Gong *et al.*, 2021).

Regular monitoring of the rice crop allows farmers to assess its growth and development, enabling them to make timely decisions to optimize yield. Monitoring of crop performance helps to identify potential issues such as nutrient deficiencies, pest and disease outbreaks, water stress, or weed infestations (Shafi *et al.*, 2019). By addressing these problems promptly, farmers can minimize yield losses and maximize the productivity of their rice crop (Bendig *et al.*, 2015; Genc *et al.*, 2013; Wang *et al.*, 2012). This ensures that the rice plants receive adequate nutrients for healthy growth, minimizing nutrient deficiencies or excesses that can affect yield and crop quality. Ongoing monitoring of the rice crop provides farmers with essential data for making informed decisions and managing risks. By having real-time information on crop health, growth, and environmental conditions, farmers can adjust their management practices, allocate resources effectively, and make informed choices about pest control, fertilization, irrigation, and other critical aspects (Garcia and Barbedo, 2019). This enables proactive management and helps mitigate potential risks and uncertainties associated with rice farming (Candiago *et al.*, 2015; Wang *et al.*, 2019).

Crop vigor and performance monitoring, including plant crop parameters like leaf chlorophyll, above ground biomass, Plant height, Leaf area Index, Leaf moisture, and yield aids in early stress detection (Bendig *et al.*, 2015). Changes in plant vigor can indicate environmental stresses, such as drought, excessive heat, or disease pressure. Timely identification of stress allows for prompt intervention and mitigation measures. By monitoring crop performance, growers can implement appropriate stress management strategies, including adjusting irrigation, modifying cultural practices, or applying treatments to mitigate the stress impact on crop vigor and performance. Assessing crop vigor and performance, contributes to yield estimation and forecasting. Healthy plants with optimal levels are more likely to achieve higher yields. But farmers do not have sufficient methods to monitor the crop performance quickly and easily other than traditional time consuming and labor intensive methods (Mandal *et al.*, 2008).

Several conventional methods are available for estimating Leaf chlorophyll content (Leaf-Chl), such as Soil Plant Analysis Development (SPAD) chlorophyll meters which are handheld devices that measure the relative chlorophyll content in leaves. Also, there are laboratory methods involves extracting chlorophyll from leaf samples (Slam *et al.*, 2009). But requires sample collection, preparation, and access to a laboratory with spectrophotometric equipment (Chithranayana and Punyawardena, 2014) And sometimes these methods may difficult when it come to a huge rice field as it is a time consuming and labor intensive method.

Above ground biomass (AGB)is closely associated with the harvestable yield where a higher AGB generally indicates a healthier and more vigorous plant (Clevers and Gitelson, 2014; Swain and Zaman, 2012). It is also an important indicator of the health of crop ecosystem (Casey, 2020; Dammalage *et al.*, 2017;) Traditionally, a variety of destructive methods have been used for estimating AGB. Popular method is the destructive or harvest method which involves cutting down all aboveground biomass within a defined area, drying it to constant weight, and then weighing it to determine biomass(Gabriel *et al.*, 2017). Destructive sampling methods require field sampling, meaning that a portion of the crop or vegetation must be physically removed from the field for analysis. A major drawback is the challenge of conducting large number of sampling in a field that may require removal of considerable amount of productive plants in field and also result in data interpolation and poor representation of the real variability of AGB in the complete rice field (Dammalage *et al.,* 2017, Ling *et al*., 2011; Yuan *et al*., 2016).

The PHt (Plant height) is a physiological measurement which has a strong positive correlation with plant biomass. Using a ruler or measuring tape, the traditional method of measuring PHt in rice entails taking a direct measurement from the plant's base to its highest point (Jackson and Somers, 1989; Yang *et al*., 2015). The disc pasture method (DPM) is indeed a tool used for estimating aboveground standing grass height (Confalonieri *et al*., 2009; Harmse *et al*., 2019).

The traditional PHt methods typically require physical samples to be collected from the field, which limits the spatial coverage of the analysis. This means that it may not be possible to assess the entire field, and only a small portion of the field may be analyzed, leading to potential errors (Devia *et al*., 2019).

LM content is important for understanding the hydration status and overall health of plants. While direct measurement of LM can be challenging, several methods involve directly measuring LM by weighing a fresh leaf sample, followed by drying the sample to remove all moisture and reweighing it to determine the dry weight. Leaf conductance, also known as stomatal conductance, is a measure of the ability of leaves to transpire water vapor (Tang *et al.*, 2022). It is influenced by LM content, and by measuring leaf conductance using specialized instruments such as porometers, one can indirectly infer the LM status. Those methods are destructive and time-consuming methods.

Traditionally, crop growth parameter estimation is based upon data collection technique from ground-based field visits. Such technique is often subjective, costly and is prone to large errors, leading to poor crop assessment and crop area estimation (Filella *et al*., 1995). Also, the obtained data may become available too late for appropriate action. At the same time, no yield estimation tools unless developed or tested locally are suitable for local use. Remote sensing techniques have the potential to provide information on agricultural crops quantitatively, instantaneously, and nondestructively over large areas (Easterday *et al.*, 2019; Tsouros *et al.*, 2019). In precision agriculture, crop condition can be monitored based on the crop parameter. In general, remote sensing is a means of obtaining and interpreting information of an object from a distance, an area phenomenon by acquiring the data using sensors or devices without physical touch (Duan *et al.*, 2019; Esposito *et al.*, 2021). In today's technological era, agricultural crop conditions such as rice can be monitored rapidly from the air. The methods can be observed using camera or sensor which is platformed on helicopter, aircraft, Unmanned Aerial Vehicle (UAV) and satellite (Dammalage *et al.*, 2017).

Crop monitoring has traditionally involved applying various direct and indirect measures of plant features, soil parameters, and environmental conditions. Previous studies highlighted some VIs which can use to monitor the crop performance, and those were derived using satellite and UAV data. Compared to satellite images, UAVs are emerging as new, viable platforms for collecting spatial data at a lower cost. Contrarily, there are few studies have been conducted (Dammalage and Shanmugam, 2018; Garcia and Barbedo, 2019) for UAV derived VIs to monitor the rice crop performance in relation different rice farming ecosystems, rice varieties and climatic conditions. Furthermore, previous research has only used widely a single VIs to estimate rice crop parameters, without comparing the performances of these combinations in various rice growing ecosystems. Nevertheless, there is insufficient studies on the application of UAV multispectral imaging for estimating rice yield and parameters that have been published in Sri Lanka. Therefore, there is a significant research gap to be filled in order to examine the accuracy of combinations of VIs produced from UAV multispectral imaging over the rice ecosystem of Sri Lanka with rice types that are used locally. On the other hand there are some researches to monitor the crop leaf water stress and mapping crop water status with multispectral UAV imagery but there is no evidence of past research work reported on identifying specific VIs which measure leaf moisture of the rice crop.

Therefore, this study was designed based on the two hypothesis, Leaf-Chl, LM, AGB, PHt and RY can estimate using VIs derived from UAV-multispectral imagery and VIs developed to estimate Leaf-Chl, LM, AGB, PHt and RY can perform similar manner across rice fields in different soils, rice varieties, weedy conditions and agronomic practices.

Thus, this study aims to evaluate the potential of monitoring Leaf-Chl, LM, AGB, PHt and RY, using a UAV based remote sensing protocol, so that the farmers and researchers can monitor the crop response during management activities real-time before the harvest. In this study the generated relationship from the data of an initial experimental field was used to find the applicability of using UAV based technique to monitor the crop performance of an ongoing farmer field.

METHODOLOGY

The experiment was conducted in two steps with ground truth data and acquired UAV imagery data, a) at a controlled rice field of variety Bg 300 to test the first hypothesis and then b) at a farmer field of rice variety Bg 374 to test the second hypothesis. Both experiments were conducted during the *Maha* season.

Field Experimental design

Initial experiment in Controlled Field

In order to test the first hypothesis that UAV-multispectral imagery can measure Leaf-Chl, AGB, PHt, LM, and RY (Figure 1) a controlled field experiment was conducted at the rice fields maintained by the Rice Research and Development Institute, Bathalagoda, Sri Lanka (7°31′53.49″N, 80°26′7.29″E). Rice variety Bg 300 was established by transplanting seedlings at a spacing (4.5 m x 3 m and 49 plants/m^2 plant density) during *Maha* season 2021/2022. The rice field had a soil type of Red-Yellow Podzolic, supplied with abundant water through cannel irrigation, and agronomic practices conducted as recommended by the Department of Agriculture (DOA, Sri Lanka). Experimental layout was adopted in the field by blocking it into four blocks of artificially created controlled fertilizer application rates to simulate variability among the rice plants in the experiment. Blocks were physically separated during land preparation by ridges of soil to avoid any surface water being contaminated from the adjoining. Then four blocks were treated with four variable nitrogen (N) fertilizer rates; 0% (0 kg/ha), 50% (112.5 kg/ha), 100% (225 kg/ha), and 150% (337.5 kg/ha), respectively of recommendation for N fertilizer for rice (Sirisena, 2013) by the Department of Agriculture (DOA), Sri Lanka. Each block was contained 640 rice plants transplanted on the same day, and for easy management, plants were arranged as subplots in a block allotting a total of 16 subplots in the total field (4 subplots x 4 blocks) (Figure 2). Ground-truth measurements were taken from quadrants (1 m^2) randomly laid over each block at panicle initiation (4 WAP), booting (6WAP), and milking stage (8 WAP).

Farmer field

This study was done to test the second hypothesis that best selected combination of VIs in the controlled field remain similar at different soil type (fine loamy to clayey, kaolinitic, and isohyperthermic), agronomic practices and rice variety or otherwise selection of VIs is influenced. Hence, the farmer fields were maintained by the farmers (from November to March 2023) located at Kinigama, Gampaha district, Western Province, in Sri Lanka (7°03'25.2"N 80°02'02.5" E). *Maha* Season was used for collecting data with Bg 374 (3 1/2 month) rice variety. The data collection was conducted at the booting stage of the rice plant as it was selected which is the optimum reproductive stage (Panday *et al.,* 2020) and shows the significant association with the growth parameters (eg. Leaf-Chl, AGB, PHt, LM, and RY) and selected VIs of the initial experimental data. The experiment was carried out in a completely randomized design (Figure 3).

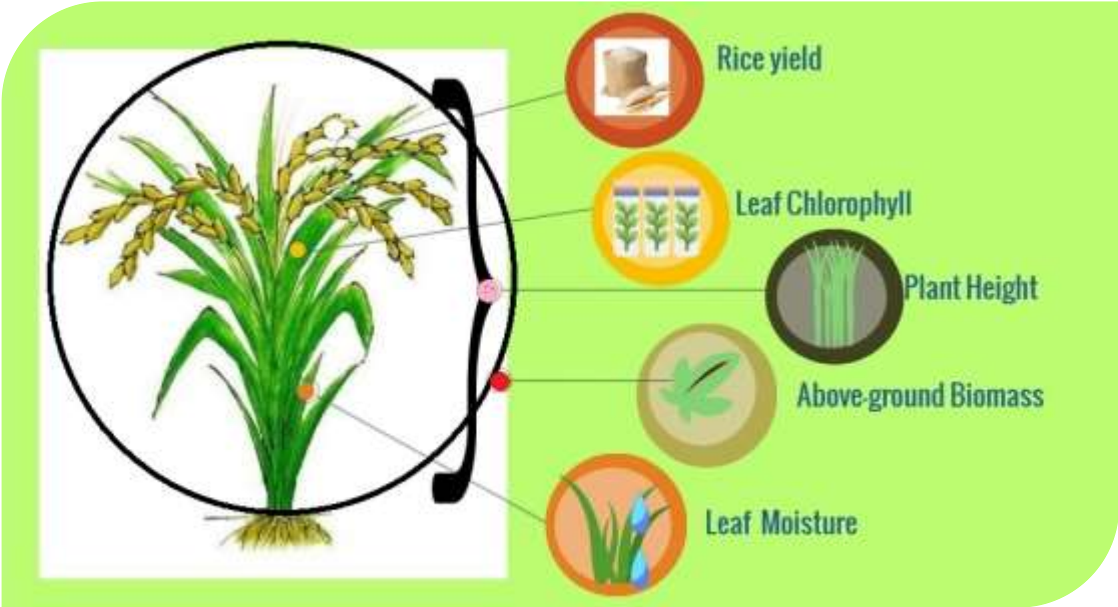

Figure 1. Measured physiological parameters of the rice crop

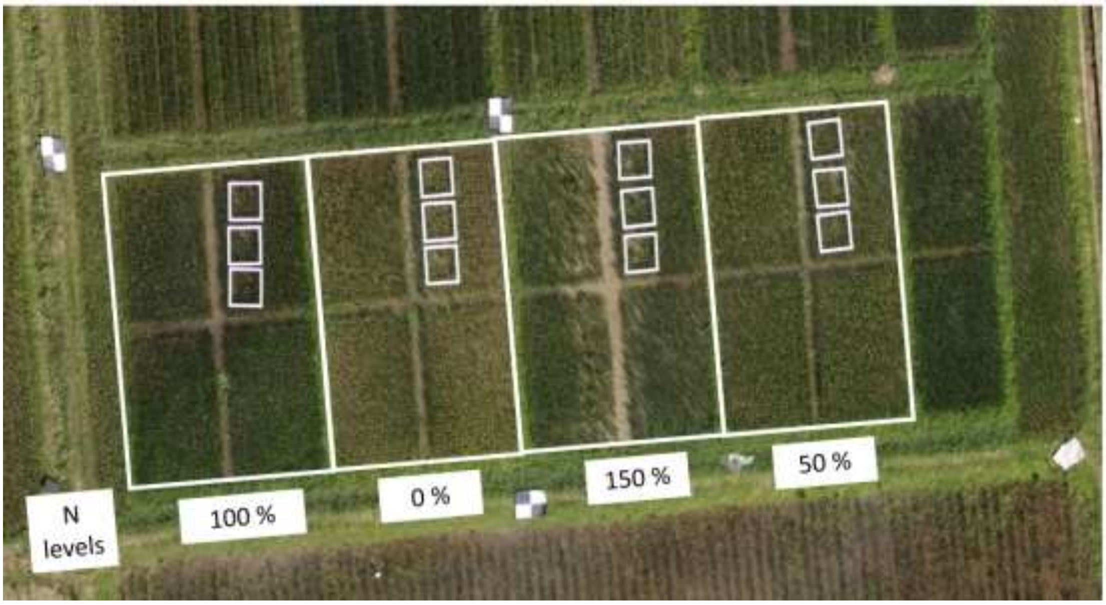

Figure 2. A sample of orthomosaic UAV captured image of the experimental rice field; showing regiform frames (marking ground sampling locations) and created known variation in the field

Ground-truth data collection

Data collection for Leaf-Chl

Leaf-Chl was measured using the SPAD–502 Chlorophyll meter (Minolta Co. Ltd., Osaka, Japan) at booting stage. Five plants were randomly selected and data was recorded on the flag leaf of each plant. Finally, the average value was recorded as the final SPAD value of the sample point (Figure 4).

Data collection for AGB

Further, destructive sampling was conducted for the calculation of AGB followed by the leaf chlorophyll measurement. Six rice plant bushes from each quadrant were uprooted and sealed in polythene bags for transportation to the laboratory within 30 min. At the laboratory soil and root parts were removed and remaining components (stem, leaves and panicle) were dried at 70 °C for 72 h, until a consistent weight was obtained (W1) (Prabhakara *et al.,* 2015). Finally, AGB was calculated as weight per unit area (kg/m^2) using Eq.1 (Casey, 2020).

$$AGB= (W1/n1) \times (n2/A) \qquad \text{(Eq.1)}$$

where,

W1=dry weight of the sample (stem, leaves and panicle of the plant), n1= No of samples taken within a 1m^2 quadrant area, n2=Total no of plants within a 1m^2 quadrant area and A= destructive above-ground biomass sampling area (1m^2).

Data collection of PHt

The disc pasture meter method was used to measure the average PHt of the rice bushes (Harmse *et al*., 2019). The meter was placed at the base of the rice plant and the disc was allowed to freely settle on the leaves as shown in Figure 5. Six readings were recorded per quadrant for the PHt (Figure 5).

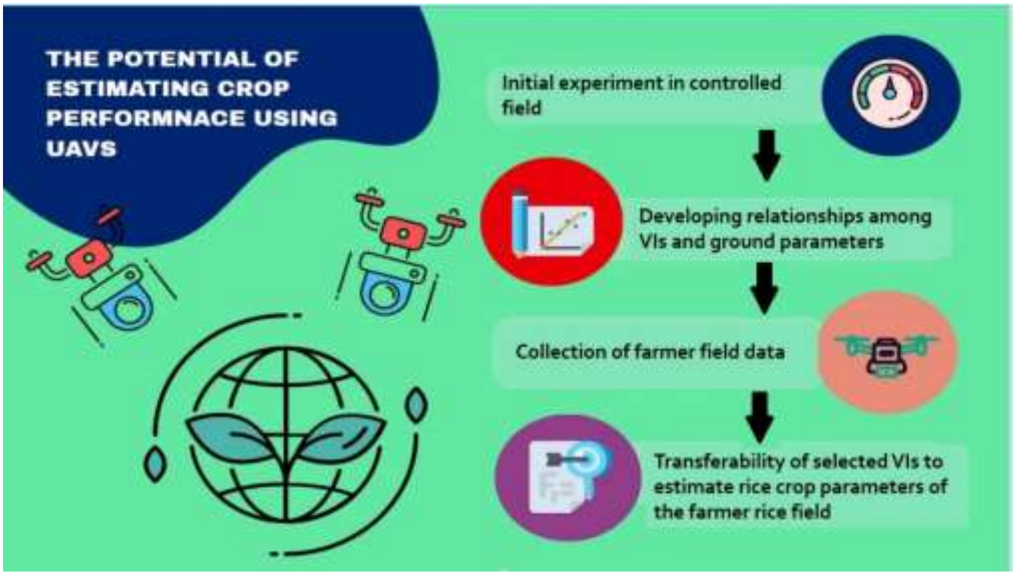

Figure 3. Flow diagram of the steps carried out in the farmer field

Figure 4. SPAD meter method used to measure Leaf Chlorophyll of the rice crop (used the fully expanded top leaf including the flag leaf from each sampling regiform quadrant)

Data collection of leaf moisture

LM measurements of rice leaves from 3 plants per quadrant were taken. The fresh mass of the sample was measured. Samples were oven-dried for 72 h at 60 °C and measured again for dry mass (Easterday *et al*., 2019). The fresh and dry mass of each sample was then used to calculate LM as (Eq. 2),(Easterday *et al*., 2019).

LM= [(Fresh mass–Dry mass)/ (Dry mass)] × 100 (Eq. 2)

Measuring actual Rice yield (RY)

Then the actual rice yield was obtained from the field before harvest using the same sampling quadrants (1m^2 quadrants). Then panicles were collected in sacks and weighed (fresh weight) and it was recorded per sample unit area (1m^2) as the actual yield for this study.

UAV aerial data collection

UAV image acquisition

Figure 6 shows the way how acquire the aerial multispectral images of the rice field using a P4 Multispectral (DJI Technology) and real time kinetic (RTK) enabled UAV (Figure 7). There are six camera sensors are mounted for capturing reflected wavebands simultaneously in blue (B): 465–485 nm, green (G): 550–570 nm, red(R): 663–673 nm, red edge (RE): 712–722 nm, and near-infrared (NIR): 820–860 nm. DJI GS Pro app was used for the mission planning by drawing a zig-zag pattern flight grid over the field with attributes; shooting angle parallel to main path, capture at equal time interval, front overlap ratio 80% and side overlap 70%. Flying height was set to 25 m with a 2 cm/px ground sampling distance (GSD). 25 m flying height was decided as the best height because an initial sensitivity test was conducted and it was found 25 m produce best results for most of the remotely measured parameters for rice (Dharmaratne *et al.*, 2024). The aerial imagery was acquired between 10:00 h to 12:00 h during sunny days when no rain.

Image processing

A single field reflectance image was generated with P4 Multispectral UAV produced multiple images using the professional photogrammetry software Pix4D mapper (Switzerland, Version 4.6.4, Perpetual licensed) software. The process included point cloud densification, orthomosaic and reflectance raster image (with correction for irradiance). Consequent B, G, R, RE, and NIR reflectance maps of the rice field were generated through this process.

Figure 5. Disc pasture method used to measure average rice plant height

Figure 6. Capturing multispectral images using the P4 Multispectral UAV over the rice field during 1.5 month before the harvest

Figure 7. Real-time kinematic (RTK) GPS guidance system

Geo-referencing

The images were geo-referenced with the RTK (Figure 7) mode enabled in the P4 Multispectral UAV.

Image segmentation

The pixels associated with non-targeted bare soil or water surfaces were removed from each raster image by segmentation, thresholding the image using its own average reflectance values from bare soil or water surfaces. This step was performed in QGIS software (Desktop 3.16.0) by following; drawn polygons on soil or water surfaces, calculated average value from the Zonal Statistics toolkit, and thresholded using Raster Calculator toolkit.

Calculation of Vis

VIs were calculated from rice crop reflectance values extracted from each sampling quadrant. The QGIS software was used to draw polygons within the quadrants in the segmented raster images to extract the average reflectance of B, G, R, RE and NIR by the Zonal Statistics toolkit. Once the extraction is completed the attribute tables were exported in MS EXCEL format to compute 20 VIs as listed in table 1.

Data analysis

The UAV derived VI responses retrieved at booting stage of rice plant were associated with ground measured rice Leaf-Chl, AGB, PHt, LM, and RY. It was evident through the Shapiro-Wilk's test that a distinct normalized variability was achievable among the rice plant growth at each growth stage during the experiment by applying different levels of N. As there were 20 indices dimension reduction was performed using partial-least-squares regression (PLS-R) in R-Studio (version 4.1.3 (2022-03-10)) analytical software to select the best fit VI or combination of VIs. The coefficient of determination (R^2) and root mean square error (RMSE) were used to assess the performances of the regression based on 20 VIs. Then the accuracy was determined with the coefficient determination values of the best fitted VIs generated by multiple linear regression analysis. Likewise, identified relationships were further extended to farmer rice fields and also new relationships were produced using farmer rice field data to compare the correlation results with controlled field results.

Table 1. Computed VIs used for this study

Index	Index ID	Formula *	Reference
Structural Indices			
Normalized Difference Vegetation Index	NDVI	(NIR- Red)/(NIR+Red)	Peng and Gitelson., (2012)
Green Normalized Difference Vegetation Index	GNDVI	(NIR-Green)/(NIR+Green)	Gitelson *et al.*,(1996)
Simple Ratio	SR	NIR/Red	Birth and McVey (1968)
Renormalized Difference Vegetation Index	RDVI	$(R_{800}- R_{670})/(R_{800}+R_{670})^{0.5}$	Roujean and Breon (1995)
Modified Simple Ratio	MSR	$(\frac{NIR}{RED}-1)/(\sqrt{\frac{NIR}{RED}}+1)$	Haboudane *et al*. (2004)
Soil Adjusted Vegetation Index	SAVI	(NIR-RED)(1+0.5)/(NIR+RED+0.5)	Huete and Naglar (1998)
Enhanced Vegetative Index	EVI	2.5(NIR-Red)/(NIR+2.4Red+1)	Birth and McVey (1968)
Normalized Green Red Vegetation Index	NGRVI	(Green-Red)/(Green+Red)	Huete and Nagler (1998)
Optimized soil-adjusted vegetation index	OSAVI	(NIR-Red)/ (NIR + Red+ 0.16)	Rondeaux *et al.* (1996)
Modified soil-adjusted vegetation index	MSAVI	$(2NIR+1-[(2NIR+1)^2-8(NIR-Red)]^{0.5})/2$	Qi *et al*., (1994)
Difference vegetation index	DVI	(NIR - Red)	Roujean and Breon (1995)
Transformed Difference Vegetation Index	TDVI	$(0.5+(NIR-Red)/(NIR+Red))^{0.5}$	Xue and Su, (2017)
Pigment Indices			
Normalized Pigment Chlorophyll Index	NPCI	$(R_{680}-R_{430}) / (R_{680}+R_{430})$	Zarco-Tejada *et al*., (2013)
Structure Insensitive Pigment Index	SIPI	$(R_{800}-R_{445})/(R_{800}+R_{680})$	Peñuelas *et al*., (1995)
Modified chlorophyll absorption in reflectance Index	MCARI	$[(R_{700}- R_{600}) -0.2(R_{700}- R_{600})](R_{700}/ R_{670})$	Borge and Leblanc (2000)
Transformed chlorophyll absorption in the reflectance index	TCARI	$3[(R_{700}- R_{670}) -2.0(R_{700}- R_{550})](R_{700}/ R_{670})$	Gitelson *et al.*,(1996)
Triangular Vegetation Index	TVI	$0.5[120(R_{750}-R_{550})-200(R_{670}-R_{550})]$	Borge and Leblanc (2000)
Chlorophyll Index Red edge	CI $_{red\ edge}$	$(R_{785}/R_{705}) -1$	Daghutry *et al*., (2000)
Normalized Difference Red edge index	NDRE	(NIR-Red edge)/ (NIR+ Red edge)	Easterday *et al*., (2019)
Green-ratio Vegetation Index	GRVI	(NIR/Green)	Sripada *et al*., (2006)

**Corresponding wavebands derived from DJI P4 Multispectral are Blue(B, R430, R445):430-495 nm, Green (G, R550): 550-580 nm, Red (R, R600, R670, R680): 600-680 nm, Red edge (RE, R700, R750): 700-750 nm, Near-Infrared (NIR, R800): 800-860 nm*

Table 2. Selected VIs from PLS-R analysis and accuracies for the estimation of Leaf-Chl by UAV

Growth stage	15 m		25 m		45 m		65 m	
	VIs	R^2	VIs	R^2	VIs	R^2	VIs	R^2
Panicle initiation stage	SIPI, GNDVI, NGRVI	0.46	NPCI, CI $_{red\ edge}$	0.44	TVI, SR, MSR	0.78	GRVI, TVI	0.79
Booting stage	MSR, CI $_{red\ edge}$	0.82	CI $_{red\ edge}$, TCARI	0.84*	CI $_{red\ edge}$, TCARI, NPCI, NDRE, MSR, NDVI	0.83	MSR, NPCI, NDVI, NGRVI	0.82
Milking stage	SR	0.68	SR	0.66	SR	0.70	SR	0.69

The mark (*) indicated the selected VI/ combination of VIs

RESULTS AND DISCUSSION

Table 2 depicted that VIs were associated with high correlation coefficient accuracy (R^2) with the booting growth stage of rice with each growth parameter. Shows a peak fit at 25 m UAV flying height whilst gradually declining when flown lower or beyond 25 m (Table 2).

Performance of growth parameters

The measured ground truth data of rice plants at controlled field, as rice crop parameters; Leaf-Chl, AGB, PHt, LM, and RY at *Maha* season were analyzed by visualizing the behavior within the artificially induced variable N levels and the normal distribution by Shapiro-Wilk's test (Confalonieri *et al.*, 2009). The normal distribution that measured Leaf-Chl, AGB, PHt, LM and rice yield values were normally distributed throughout the experiment.

Selection of VIs for Rice at controlled rice field

The results of the initial experiment carried out at the controlled rice field to test the first hypothesis are shown in following sections.

Selection of VIs for the estimation of rice Leaf-Chl, AGB, PHt, LM, RY by UAV

The selected VIs for the estimation of rice Leaf-Chl and their accuracies are listed in Table 3. Accordingly, the highest accuracy (R^2 = 0.84, RMSE= 0.28) was reported in the Booting stage (BS). Most contributed VIs were CI $_{\text{red edge}}$ and TCARI. When comparing the selected VIs associated with AGB of rice, the highest accuracy (R^2 = 0.81, RMSE= 0.06 kg/m^2) was reported for the regression model as TVI and SR. The selected VIs for the measurement of PHt and their accuracies are listed in Table 3. It shows (R^2= 0.63, RMSE= 0.11 cm) by UAV P4 multispectral images captured at 25 m. The most contributed VIs were; TVI, GRVI, and SR. The selected VIs associated with LM and their accuracies are listed in Table 3. It shows (R^2= 0.57, RMSE= 0.16%) by UAV P4 multispectral images captured at 25 m. The most contributed VIs were; TVI, and NPCI. The actual RY, harvested end of the cropping period was able to be estimated prior in the BS strongly (R^2= 0.98, RMSE= 128.5 kg/ha) by UAV P4 multispectral images captured at 25 m. The most contributed VIs were; NDVI, SIPI, GRVI, NGRVI, TCARI, CI red edge, OSAVI, and NPCI.

Validation of selected VIs to farmer rice field

In order to test the transferability of the VIs selected from the controlled field experiment, VIs were applied over the farmer rice field with fresh ground-truth data. This was done in order to test the second hypothesis that the derived VIs from UAV multispectral images can perform similar manner across rice fields in different soils, rice varieties, weedy conditions, agronomic practices, and cropping seasons. The selected optimum VIs at the controlled rice field during *Maha* were extracted from the images acquired from farmer rice fields at 25 m flying height and correlated with the freshly sampled ground-truth data from the farmer rice field itself.

Table 3. Linear regression generated for rice Leaf-Chl, AGB, PHt, LM, and RY

Growth parameter/RY	R^2	RMSE	Mean	Standard deviation
Leaf-Chl	0.84	0.28	36.52	2.79
AGB	0.81	0.06 kg/m^2	0.98 kg/m^2	0.13
PHt	0.63	0.11 cm	51.01 cm	3.22
LM	0.57	0.16%	44.06 %	2.89
RY	0.98	128.5 kg/ha	4622.9 kg/ha	701.89

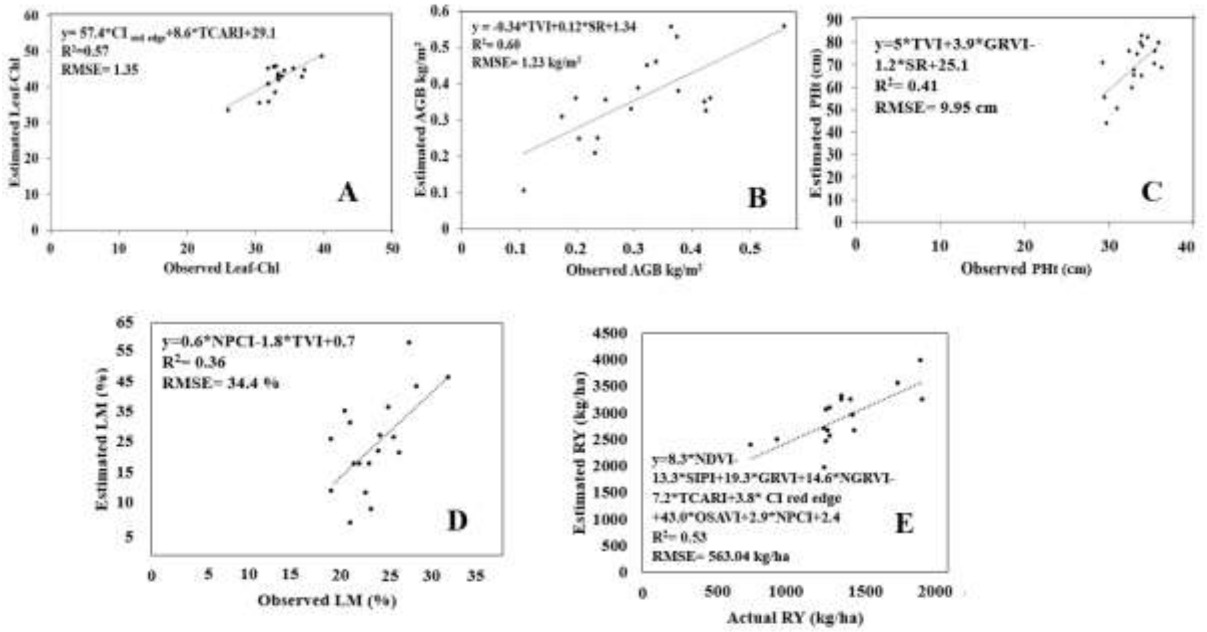

Figure 8. Scatter plots showing the associations produced by transferring optimum VIs over farmer field: (A) Estimated Leaf-Chl vs observed Leaf-Chl, (B) Estimated AGB vs observed AGB, (C) Estimated PHt vs observed PH, (D) Estimated LM vs observed LM, and (E) Estimated RY vs Actual RY at farmer rice field

The accuracy of the correlation between observed and estimated Leaf-Chl is R^2=0.57 and RMSE=1.35 (Figure 8A). However, the results show a drop in the accuracies from R^2 =0.84 to R^2 =0.57 due to the varying field/soil conditions, crop variety, and weedy conditions that existed in the farmer rice field.

The best performing VI or combination of VIs (TVI and SR) show cumulative adjusted R^2=0.81 at the initial experiment (Table 3). Next, the derived correlation using that VIs were used to estimate the AGB content in the farmer rice field. The accuracy of the correlation between observed and estimated AGB is R^2=0.60 and RMSE=1.23 kg/m^2 (Figure 8B).

When the PHt was estimated in the farmer field using VIs selected from the controlled field also showed a decrease in accuracy as R^2=0.63 to R^2=0.41 (Figure 8C).

When the LM was estimated in farmer field conditions using VIs selected from the controlled field, show adjusted R^2=0.57 at the initial experiment. Next, the derived relationship using VIs was used to estimate the LM of the rice leaves of the farmer field. The accuracy of the correlation between observed and estimated LM is R^2=0.36 and RMSE=34.4% (Figure 8D). It also shows a low correlation at the farmer field level data

When the AGB was estimated in farmer field conditions using VIs selected from the controlled field, shows adjusted R^2=0.98 in the initial experiment. Next, the derived relationship using VIs was used to estimate the RY of the farmer field. The correlation between observed and estimated RY is R^2=0.53 and RMSE=563.04 kg/ha (NDVI, SIPI, GRVI, NGRVI, TCARI, CI $_{red\ edge}$, OSAVI, and NPCI) (Figure 8E).

Re-applying PLS-R analysis over farmer rice fields

In order to select the optimum VIs associated with farmer rice field condition, the PLS-R analysis was performed again over the ground-truth data and UAV-derived VIs from farmer rice field. The VIs selected for rice crop parameters using PLS-R analysis over farmer rice fields during *Maha* season. The results depicted that VIs selected for rice crop parameters at farmer field are different from the VIs selected for rice crop parameters from controlled field during *Maha* season (Table 4).

The spectral data such as VIs derived from UAV-based images can be used for rice yield estimation (Shafian *et al.*, 2018).The association of SPAD value and AGB and UAV-based VIs values during the middle of the reproductive period suggested that UAV-based VIs can be a good alternative for field measured physiological parameters, which was stable with aforementioned studies (Bendig *et al.,* 2015).

In addition, the close associations between UAV-based VIs and Leaf-Chl have been highlighted in many studies. Clevers and Gitelson, (2014)found that CI $_{red\ edge}$ index is an accurate and linear estimator of Leaf-Chl using satellite. TCARI was identified as the pigment index (Haboudane *et al*., 2002)which is positively correlate with the Leaf-Chl. Consequently, in this study, highlighted the cumulative adjusted R^2 of the CI $_{red\ edge}$ and TCARI at booting stage using UAV data. However, the developed relationship for Leaf-Chl (Table 1) was used to estimate Leaf-Chl against the Leaf-Chl measurement from commercial farmer field. However, when applying the VIs to the farmer field the drop of the accuracies from R^2 =0.84 to R^2 =0.57 is due to the varying field condition and crop variety existed in the commercial farmer field. On the other hand, results proved that the combination of VIs selected for the estimation of rice Leaf-Chl was possible to estimate the rice Leaf-Chl across different field/soil conditions, rice varieties and weedy conditions at reasonable accuracy.

Prabhakara *et al*., (2015) highlighted in their study that VIs was not applicable to estimate AGB of the barley and rye when there is high vegetation but in this study combination of TVI and SR was identified as the positively correlated for estimation of AGB of the rice crop at the booting stage (R^2>0.8). For instance, the correlation between observed and estimated AGB shows R^2=0.60 in this study, so the low accuracy may due to the varying field condition, for instance, under high-density planting and weedy condition at the farmer field level, rice plants may have lower AGB due to competition for resources and crop variety existed in the commercial farmer field.

The estimated PHt is in good agreement with the measured PHt over the booting stage (R^2=0.63, RMSE=0.11 cm, TCARI). In this study, the correlation between observed and estimated PHt and the spectral indices from multispectral images were studied at booting stages based on images taken by a UAV. Results showed that the spectral indices of the booting stage had low significant correlation (R^2>0.4). However, in this study the correlation between PHt estimations and ground measurements was weak may be due to lack of structural or height specific information containing in the VIs. Therefore, it would be useful to check on alternative possibility of relating the plant height specific data maybe derived from the Plant Height Model (PHM) developed from the Multispectral images (Hassan *et al.*, 2019).

Table 4. The R^2 and RMSE values obtained for selected optimum VIs by re-applying PLS-R analysis over famer rice field during *Maha* season

Rice crop parameters	VI/Combination of VIs	R^2	RMSE
Leaf-Chl	GNDVI, MSAVI, CI $_{red\ edge}$, EVI	0.52	2.28
AGB	NDRE	0.58	1.99 kg/m^2
PHt	MSAVI	0.40	8.82 cm
LM	GRVI, TVI	0.18	4.81%
RY	SR, GRVI, MSR, NPCI	0.97	228.5 kg/ha

Reuben *et al.*, (2021) depicted the feasibility of UAV-based multispectral imaging for canopy water status assessment of African eggplant (*Solanum aethopicum* L.). They have shown that the single VI which correlated with LM (NDVI or OSAVI). Therefore, in this study there are combination of VIs which has shown significant correlation at the initial experiment (R^2>0.5), but when it comes to the comparison with the farmer field data it has shown low accuracy (R^2=0.36, RMSE= 3.44%) between observed and estimated LM at the field level experiment. It may due to the uncertainty of farmer level (e.g., soil moisture profile), and the varying field condition and crop variety existed in the commercial farmer field.

It has to be mentioned that relationship between grain yield and VIs shown higher accuracy at booting stage (R^2= 0.98). Therefore, this study shows that the combination of NDVI, SIPI, GRVI, NGRVI, TCARI, $CI_{red\ edge}$, OSAVI, and NPCI can be used to estimate the rice grain yield (6 weeks prior to harvest) 1.5 month before the harvest. It means in this combination there are 2 structural indices (NDVI and OSAVI), and 6 pigment indices (SIPI, GRVI, NGRVI, TCARI, $CI_{red\ edge}$, and NPCI) which represent the absorption spectra of the most important leaf pigments (Gabriel *et al*., 2017). Previously published results indicated that the booting stage could provide higher estimation accuracy when using VIs to estimate rice yield (Zhou *et al*., 2017), *Duan et al.*, (2019) also successfully estimated rice yield using reflectance measured at booting stage, which is consistent with the results from this study. Thus, the booting stage (1 ½ month before the harvest) may be the best period and the boundary point for the estimation of grain yield in rice.

The coefficient of determination of the relationship between the observed and estimated RY was R^2=0.53 and RMSE=563.04 kg/ha which is a low estimation accuracy. However, drop of the accuracies from R^2 =0.98 to R^2 =0.53 is due to the variation across rice fields in different soils, rice varieties, weedy conditions, agronomic practices existed in the commercial farmer field. On the other hand, accuracies proved that the relationship was possible to estimate the RY across different field/soil conditions, rice varieties and weedy conditions (Kaivosoja *et al*., 2021).

Additionally, this study was used PLS-R analysis to extract VIs from the farmer field data to generate the field specific VIs. It has shown significant accuracy for each parameter as it was applied PLS-R individually for the each growth parameter to extract VIs (R^2=0.52, R^2=0.58, R^2=0.40, R^2=0.31, R^2=0.18, and R^2=0.97 during *Maha* season). So there are different VIs selected when the analysis applied to the farmer field individually. Controlled fields are often carefully controlled environments that can manipulate various factors, such as water availability, nutrient levels, and pest control (Genc *et al.,* 2013). In contrast, farmer fields may exhibit greater variability due to differences in management practices, soil types, and local conditions. Farmers may employ diverse management practices based on their local knowledge, resources, and preferences. These practices can influence vegetation growth, health, and responses to environmental conditions.

One of the challenges encountered in this research was the possibility that the multispectral imagery's field reflectance was impacted by weeds leaf overlapping on farmer fields. Using extended image analysis techniques, such as leaf texture-based techniques, to separate the rice and weed leaves from the image could be one approach to get around issue (Gitelson and Merzlyak, 1996; Gong *et al*., 2021). Also there is another barrier in this study was the lack of easy access to the laboratory facilities to analyze the ground truth measurement of rice leaf moisture at commercial farmer field samples as they need to analyze quickly before the changes of leaf moisture content.

The study should be expanded further to include a large number of sample points from commercial farmer fields in a variety of ecosystems and climatic situations. These will be used for data testing and training purposes, and the best VIs will be chosen for use in future model development work.

Moreover, this study suggested that UAV-based remote sensing can acquire a huge dataset at the same time, which affords a more complete outline of rice growth by joining diverse image parameters. Reported studies has established that spectral VIs extracted from UAV based multispectral images were connected to crop productivity (Stavrakoudis *et al.*, 2019).

In general, the tendency of NDVI, GRVI, NGRVI, and NPCI (Filella *et al.*, 1995; Nebiker *et al.*, 2016) SIPI, TCARI, CI $_{\text{red edge}}$ and OSAVI (Devia *et al.,* 2019; Panday *et al.,* 2020)extracted from the multispectral camera in this study was reliable with that in past studies which have explained that these VIs individually can be used to estimate actual rice grain yield.

CONCLUSION

The findings from this study suggest that crop remote sensing technology can be used as a surrogate for traditional subjective crop monitoring methods in rice fields. According to the results, we can show that the VIs derived from UAV-multispectral imagery depict a significant correlation with observed Leaf-Chl, AGB, PHt, and RY data though there is an low accuracy for estimation of LM and VIs LM estimation may effect with rice fields in different soils, rice varieties, weedy conditions and agronomic practices.

Though low accuracies tend to be achieved when a common set of Vis are used for measuring Leaf-Chl, AGB, and RY, respectively, across different fields, the accuracies can improve when Vis are derived field-specific/ Vis by re-applying PLS-R analysis over famer rice field. Where specially RY can be improved up to $R^2 > 0.90$, with combinations of SR, GRVI, MSR, and NPCI in highly variable farmer field conditions. UAV-based multispectral imagery were capable of estimate rice crop growth parameters and rice yield with high accuracy and can be used to estimate those parameters 1 ½ month before the harvest encouraging more environmental sustainable agriculture.

ACKNOWLEDGEMENTS

The author acknowledge the kind help given by Mr. R.P.P.S. Rathnayake.

REFERENCES

Agudo, P. U., Ang, J., Fernando, P. and Ezquerra, B. (2018). The Potential of Drones and Sensors to Enhance Detection of Archaeological Cropmarks : A Comparative Study Between Multi-Spectral and Thermal Imagery. *Drones*, *2*, 1–23. https://doi.org/10.3390/drones2030029

Bendig, J., Yu, K., Aasen, H., Bolten, A., Bennertz, S., Broscheit, J., Gnyp, M. L. and Bareth, G. (2015). Combining UAV-based plant height from crop surface models , visible , and near infrared vegetation indices for biomass monitoring in barley. *International Journal of Applied Earth Observations and Geoinformation*, *39*, 79–87. https://doi.org/10.1016/j.jag.2015.02.012

Birth, G. S. and McVey, G. (1968). Measuring the colour growing turf with a reflectance spectroradiometer. Agronomy Journal 60, 640-643.

Borge, N. H. and Leblanc, E. (2000). Comparing prediction power and stability of broadband and hyperspectral vegetation indices foe estimation of green leaf area index and canopy chlorophyll density. Remote sensing of Environment 76, 156-172.

Candiago, S., Remondino, F., Giglio, M. De, Dubbini, M. and Gattelli, M. (2015). Evaluating Multispectral Images and Vegetation Indices for Precision Farming Applications from UAV Images. *Remote Sens*, *Vi*, 4026–4047. https://doi.org/10.3390/rs70404026

Casey, B. N. (2020). *Leaf angle and leaf stomata responses to experimental drought in Quercus velutina and Acer saccharum Department of Geology and Geography*. Eberly College of Arts and Sciences at West Virginia University.

Chithranayana, R. D. and Punyawardena, B. V. R. (2014). Adaptation to the vulnerability of paddy cultivation to climate change based on seasonal rainfall characteristics. *Journal of the National Science Foundation of Sri Lanka*, *42*(2), 119–127.

Clevers, J. G. P. W. and Gitelson, A. A. (2014). Remote estimation of crop and grass chlorophyll and nitrogen content using red-edge bands on Sentinel-2 and -3. *International Journal of Applied Earth*

Observations and Geoinformation, *23*(2013), 344–351. https://doi.org/10.1016/j.jag.2012.10.008

Confalonieri, R., Rosenmund, A. S. and Baruth, B. (2009). An improved model to simulate rice yield. *Agron. Sustain. Dev*, *29*, 463–474. https://doi.org/DOI: 10.1051/agro/2009005

Daghutry, C. S. T. (2000). Estimating corn leaf chlorophyll con-centration from leaf and canopy reflectance. Remote sensing of Environment 5, 231-233.

Dammalage, T. L., Sirisena, P. M. T. S. and Susaki, J. (2017). MODIS Satellite Data Based Rice Yield Forecasting Model for Sri Lanka: A Pilot Study in Kurunegala District. *Asian Journal of Geoinformatics*, *17*, 25–40. http://edc.usgs.gov/

Dammalage, T. and Shanmugam, T. (2018). *Use of Satellite Remote Sensing for Rice Yield Estimation : A Case Study of Polonnaruwa District , Sri Lanka*. *7*(4), 1–9. https://doi.org/10.9734/AJAAR/2018/43843

Devia, C. A., Rojas, J. P., Carol, E. P., Ivan, M., Patino, F. M. D. and Colorado, J. (2019). High-Throughput Biomass Estimation in Rice Crops Using UAV Multispectral Imagery. *Journal of Intelligent and Robotic Systems*, 1–19. https://doi.org/https://doi.org/10.1007/s10846-019-01001-5 High-Throughput

Dharmaratne, P. P., Salgadoe, A. S. A. and Rathnayake, W. M. U. K. (2024). Remote Sensing Applications : Society and Environment Estimating rice crop (Oryza sativa L .) parameters during the ' Yala ' season in Sri Lanka using UAV multispectral indices. *Remote Sensing Applications: Society and Environment*, *33*(July 2023), 101132. https://doi.org/10.1016/j.rsase.2023.101132

Duan, B., Fang, S. and Zhu, R. (2019). Remote Estimation of Rice Yield With Unmanned Aerial Vehicle (UAV) Data and Spectral Mixture Analysis. *Frontiers in Plant Science*, *10*, 1–14. https://doi.org/10.3389/fpls.2019.00204

Easterday, K., Kislik, C., Dawson, T. E., Hogan, S. and Kelly, M. (2019). *Remotely Sensed Water Limitation in Vegetation : Insights from an Experiment with Unmanned Aerial Vehicles (UAVs)*. 1–18.

Esposito, M., Crimaldi, M., Cirillo, V., Sarghini, F. and Maggio, A. (2021). Drone and sensor technology for sustainable weed management : a review. *Chemical and Biological Technologies in Agriculture*, 1–11. https://doi.org/10.1186/s40538-021-00217-8

Filella, I., Serrano, L., Serra, J. and Penuelas, J. (1995). Evaluating Wheat Nitrogen Status with Canopy Reflectance Indices. *Crop Sci*, *35*, 1400–1405.

Gabriel, J. L., Zarco-Tejada, P. J. and López-Herrera, P. J. (2017). Airborne and ground level sensors for monitoring nitrogen status in a maize crop. *Biosystems Engineering*, *160*, 124–133. https://doi.org/10.1016/j.biosystemseng.2017.06.003

Garcia, J. and Barbedo, A. (2019). *A Review on the Use of Unmanned Aerial Vehicles and Imaging Sensors for Monitoring and Assessing Plant Stresses*. https://doi.org/10.3390/drones3020040

Genc, L., Inalpulat, M., Kizil, U., Mirik, M., Smith, S. E. and Mendes, M. (2013). Determination of water stress with spectral reflectance on sweet corn (Zea mays L .) using classification tree (CT) analysis. *Zemdirbyste-Agriculture*, *100*(1), 81–90. https://doi.org/10.13080/z-a.2013.100.011

Gitelson, A. A. and Merzlyak, M. N. (1996). Signature Analysis of Leaf Reflectance Spectra : Algorithm Development for Remote Sensing of Chlorophyll. *Journal of Plant Physiology*, *148*(3–4), 494–500. https://doi.org/10.1016/S0176-1617(96)80284-7

Gong, Y., Yang, K., Lin, Z., Fang, S., Wu, X., Zhu, R. and Peng, Y. (2021). Remote estimation of leaf area index (LAI) with unmanned aerial vehicle (UAV) imaging for different rice cultivars throughout the entire growing season. *Plant Methods*, 1–16. https://doi.org/10.1186/s13007-021-00789-4

Haboudane, D., Miller, J. R., Tremblay, N., Zarco-tejada, P. J. and Dextraze, L. (2002). Integrated narrow-band vegetation indices for prediction of crop chlorophyll content for application to precision agriculture. *Remote Sensing of Environment*, *81*, 416–426.

Harmse, C. J., Dreber, N. and Trollope, W. S. W.

(2019). Disc pasture meter calibration to estimate grass biomass production in the arid dunefield of the south-western Kalahari. *African Journal of Range and Forage Science*, *36(3)*, 161–164. https://doi.org/10.2989/10220119.2019.1610905

Hassan, M. A., Yang, M., Fu, L., Rasheed, A., Zheng, B., Xia, X., Xiao, Y. and He, Z. (2019). Accuracy assessment of plant height using an unmanned aerial vehicle for quantitative genomic analysis in bread wheat. *Plant Methods*, *15*(1), 1–12. https://doi.org/10.1186/s13007-019-0419-7

Huete, A. R., and Naglar, P. L. (1998). Assessment of spectral vegetation Indices for riparian vegetation in the Colorado River delta, Mexico. Journal of Arid Environments 49, 91-110.

Jackson, T. A. and Somers, G. F. (1989). Direct and indirect methods for estimating tree height and basal area. *Forest Ecology and Management*, *27(4)*, 265-272. https://doi.org/10.1016/j.smrv.2018.05.005

Jiang, Q., Fang, S. and Peng, Y. (2019). UAV-Based Biomass Estimation for Rice-Combining Spectral , TIN-Based Structural and Meteorological Features. *Remote Sensing*, *11*, 1–19. https://doi.org/doi:10.3390/rs11070890

Kaivosoja, J., Hautsalo, J., Heikkinen, J., Hiltunen, L., Ruuttunen, P., Näsi, R., Niemeläinen, O., Lemsalu, M., Honkavaara, E. and Salonen, J. (2021). Reference Measurements in Developing UAV Systems for Detecting Pests , Weeds , and Diseases. *Remote Sensing*, *13*.

Ling, Q., Huang, W. and Jarvis, P. (2011). Use of a SPAD-502 meter to measure leaf chlorophyll concentration in Arabidopsis thaliana. *Plant Physiology and Ecology*, *2*, 1–14.

Mandal, U. K., Singh, K. K. and Singh, M. N. (2008). Improvement in the method of grain yield estimation in rice. *International Rice Research Notes*, *29(2)*, 31–32. https://ink.library.smu.edu.sg/soe_research Part

Nebiker, S., Lack, N., Abächerli, M. and Läderach, S. (2016). LIGHT-WEIGHT MULTISPECTRAL UAV SENSORS AND THEIR CAPABILITIES FOR PREDICTING GRAIN YIELD AND DETECTING PLANT DISEASES. *Remote Sensing and Spatial Information Sciences, XLI*(July), 12–19. https://doi.org/10.5194/isprsarchives-XLI-B1-963-2016

Nordh, N. and Verwijst, T. (2004). Above-ground biomass assessments and first cutting cycle production in willow (Salix sp .) coppice — a comparison between destructive and non-destructive methods. *Biomass and Bioenergy*, *27*, 1–8. https://doi.org/10.1016/j.biombioe.2003.10.007

Panday, U. S., Pratihast, A. K. and Aryal, J. (2020). A Review on Drone-Based Data Solutions for Cereal Crops. *Drones*, *4*(41), 1–29.

Prabhakara, K., Dean Hively, W. and McCarty, G. W. (2015). Evaluating the relationship between biomass, percent groundcover and remote sensing indices across six winter cover crop fields in Maryland, United States. *International Journal of Applied Earth Observation and Geoinformation*, *39*, 88–102. https://doi.org/10.1016/j.jag.2015.03.002

Peng, Y., and Gitelson, A. A. (2012). Remote estimation of gross primary productivity in soybean and maize based on total crop chlorophyll content. Remote Sensing of Environment 117,440–448

Peñuelas, J., Filella, I., and Gamon, J.A. (1995). Assessment of photosynthetic radiation-use efficiency with spectral reflectance. New Phytol. 131, 291–296.

Qi, J., Chehbouni, A., Huete, A.R., Kerr, Y.H., and Sorooshian, S. (1994). A modified soil adjusted vegetation index. Remote Sens. Environ. 48, 119–126, http://dx.doi.org/10.1016/0034-4257(94)90,134-1.

Reuben, P., Mbilinyi, B. P., Mbungu, W. B., Mourice, S. K., Mahoo, H. F. and Schmitter, P. (2021). The feasibility of hand-held thermal and UAV-based multispectral imaging for canopy water status assessment and yield prediction of irrigated African eggplant (Solanum aethopicum L). *Agricultural Water Management*, *245*, 106584. https://doi.org/10.1016/j.agwat.2020.106584

Rondeaux, G., Steven, M., and Baret, F. (1996). Optimization of soil-adjusted vegetation indices. Remote Sens. Environ. 55, 95–107, http://dx.doi.org/10.1016/0034-4257

Roujean, J.L., and Breon, F.M. (1995). Estimating PAR absorbed by vegetation from bidirectional reflectance measurements. Remote Sens. Environ 51, 375–384.

Shafi, U., Mumtaz, R., García-Nieto, J., Hassan, S. A., Zaidi, S. A. R. and Iqbal, N. (2019). Precision agriculture techniques and practices: From considerations to applications. *Sensors (Switzerland)*, *19*(17), 1–25. https://doi.org/10.3390/s19173796

Shafian, S., Rajan, N., Schnell, R., Bagavathiannan, M., Valasek, J., Shi, Y. and Olsenholler, J. (2018). Unmanned aerial systems-based remote sensing for monitoring sorghum growth and development. *PLoS ONE*, *13*(5). https://doi.org/10.1371/journal.pone.0196605

Slam, M. S. I., Huiya, M. S. U. B. and Ahman, S. R. (2009). Evaluation of spad and lcc based nitrogen management in rice (*Oryza sativa* L.). *Bangladesh J. Agril. Res*, *34*(4), 661–672.

Sripada, R.P., Heiniger, R.W., White, J.G., Meijer, A.D. (2006). Aerial color infrared photography for determining early in-season nitrogen requirements in corn. Agron. J. 98, 968-971.

Stavrakoudis, D., Katsantonis, D. and Kadoglidou, K. (2019). Estimating rice agronomic traits using drone-collected multispectral imagery. *Remote Sensing*, *11*(5), 545–570. https://doi.org/10.3390/rs11050545

Swain, K. C. and Zaman, Q. U. (2012). Rice Crop Monitoring with Unmanned Helicopter Remote Sensing Images. *Remote Sensing of Biomass*, *3*, 253–272. www.intechopen.com

Tang, Z., Jin, Y., Alsina, M. M., McElrone, A. J., Bambach, N. and Kustas, W. P. (2022). Vine water status mapping with multispectral UAV imagery and machine learning. *Irrigation Science*, *40*(4–5), 715–730. https://doi.org/10.1007/s00271-022-00788-w

Tsouros, D. C., Bibi, S. and Sarigiannidis, P. G. (2019). A review on UAV-based applications for precision agriculture. *Information (Switzerland)*, *10*(11). https://doi.org/10.3390/info10110349

Verwijst, T. and Telenius, B. (1999). Biomass estimation procedures in short rotation forestry. *Forest Ecology and Management*, *121*, 137–146.

Wang, P., Chen, S. H., Chang, K. W. and Shen, Y. (2012). Identifying and characterizing yield limiting factors in paddy rice using remote sensing yield maps. *Precision Agriculture*, *13*(5), 553–567. https://doi.org/10.1007/s11119-012-9266-5

Wang, Y., Zhang, K., Tang, C., Cao, Q., Tian, Y., Zhu, Y., Cao, W. and Liu, X. (2019). Estimation of rice growth parameters based on linear mixed-effect model using multispectral images from fixed-wing unmanned aerial vehicles. *Remote Sensing*, *11*(11). https://doi.org/10.3390/rs11111371

Xue, J. and Su, B. (2017). Significant remote sensing vegetation indices : a review of developments and applications. Sensors 3, 1–17. doi: https://doi.org/10.1155/2017/1353691 Review.

Yang, L., Yang, R. and Meng, Q. (2015). Comparison of direct and indirect methods for measuring plant height in wheat. *Crop Science*, *55(4)*, 1522–1528.

Yuan, Z., Cao, Q., Zhang, K., Ata-ul-karim, S. T., Tian, Y. and Zhu, Y. (2016). *Optimal Leaf Positions for SPAD Meter Measurement in Rice*. *7*(May), 1–10. https://doi.org/10.3389/fpls.2016.00719

Zarco-Tejada, P. J., Morales, A., Testi, L. and Villalobos, F. J. (2013). Spatio-temporal patterns of chlorophyll fluorescence and physiological and structural indices acquired from hyperspectral imagery as compared with carbon fluxes measured with eddy covariance. *Remote Sensing of Environment*, *133*, 102–115. https://doi.org/http://dx.doi.org/10.1016/j.rse.2013.02.003

Zhou, X., He, J. and Zheng, H. (2017). Predicting grain yield in rice using multi-temporal vegetation indices from UAV-based multispectral and digital imagery. *ISPRS Journal of Photogrammetry and Remote Sensing*, *130*, 246–255. https://doi.org/10.1016/j.isprsjprs.2017.05.003